Automatic Brain Segmentation in Rhesus Monkeys

Martin Styner[a,b], Rebecca Knickmeyer[b], Sarang Joshi[c], Christopher Coe[d], Sarah J Short[d], John Gilmore[b]

[a]Department of Psychiatry, University of North Carolina, Chapel Hill NC, USA;
[b]Department of Computer Science, University of North Carolina, Chapel Hill NC,USA
[c]Department of Biomedical Engineering, University of Utah, Salt Lake City, Utah, USA
[d]Department of Psychology, University of Wisconsin, Madison, WI, USA

ABSTRACT

Many neuroimaging studies are applied to primates as pathologies and environmental exposures can be studied in well-controlled settings and environment. In this work, we present a framework for both the semi-automatic creation of a rhesus monkey atlas and a fully automatic segmentation of brain tissue and lobar parcellation. We determine the atlas from training images by iterative, joint deformable registration into an unbiased average image. On this atlas, probabilistic tissue maps and a lobar parcellation. The atlas is then applied via affine, followed by deformable registration. The affinely transformed atlas is employed for a joint T1/T2 based tissue classification. The deformed atlas parcellation masks the tissue segmentations to define the parcellation. Other regional definitions on the atlas can also straightforwardly be used as segmentation.

We successfully built average atlas images for the T1 and T2 datasets using a developmental training datasets of 18 cases aged 16-34 months. The atlas clearly exhibits an enhanced signal-to-noise ratio compared to the original images. The results further show that the cortical folding variability in our data is highly limited. Our segmentation and parcellation procedure was successfully re-applied to all training images, as well as applied to over 100 additional images. The deformable registration was able to identify corresponding cortical sulcal borders accurately.

Even though the individual methods used in this segmentation framework have been applied before on human data, their combination is novel, as is their adaptation and application to rhesus monkey MRI data. The reduced variability present in the primate data results in a segmentation pipeline that exhibits high stability and anatomical accuracy.

1. INTRODUCTION

Neuroimaging studies are increasingly applied to primates as pathologies and environmental exposures can be studied in well-controlled settings and environment. In our own current studies, we are investigating the neurological brain development in rhesus monkeys (Macaca mulatta) in regard to various adverse exposure models such as prenatal, intrauterine exposure to auditory stress or maternal flu-infection. The employed measurements in those studies include brain tissue volume, lobar parcellation, as well structural segmentations. In this paper we present a framework that provides a solution to all of the these measurements.

Another line of primate brain analysis has been introduced and promoted by Van Essen et al,[1–6] which focuses on the surface based analysis of the macaque cerebral cortex and its parcellation into cognitive areas. This type of analysis is complementary to ours as it allows the direct investigation of cortical surface parcellation. On the other hand our methods offer cortical properties (such as cortical thickness), white matter parcellation, and subcortical structures properties. These measurements can be employed in combination with the surface based methodology to compare local cortical properties, such as cortical thickness.[7,8]

In this article, we present a novel framework for the atlas based tissue segmentation, followed by lobar parcellation. In the next section, the different steps in our framework are detailed, starting with the generation of the atlas, as well as the application of the atlas to rhesus monkey datasets in a series of steps based on tools originally developed for use with human MRI studies.

Email: martin_styner@ieee.org, WWW: www.ia.unc.edu

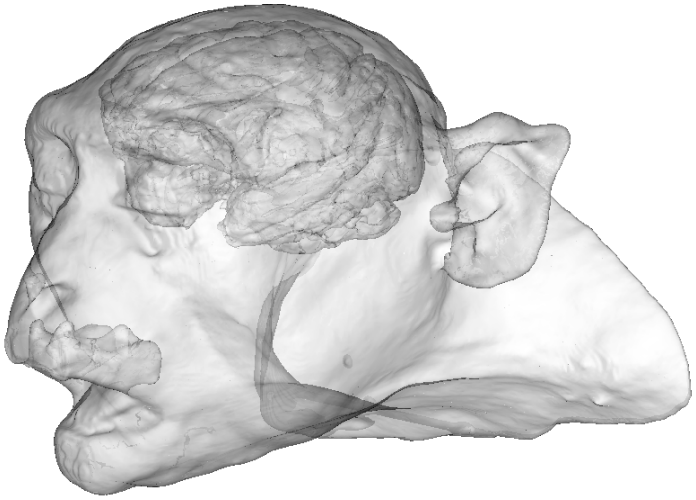

Figure 1. Illustration of brain segmentation with corresponding skin segmentation of an example MRI dataset in our studies of rhesus monkey brain development (both skin and brain surface are transparent).

2. METHODS

We have developed a framework for both the semi-automatically creation of an rhesus monkey brain atlas and automatic atlas based brain segmentation. The framework consists of 2 main steps: atlas building and application. In the atlas building step, we determine an unbiased atlas image from a set of training images after a series of preprocessing steps. On this atlas we define a probabilistic tissue segmentation, as well as a lobar parcellation. Using existing tools developed for human MRI use, we apply the atlas to determine tissue segmentations and lobar parcellation.

2.1. Subjects and Datasets

In our target studies we are studying brain development in rhesus monkeys using a single atlas. For the computation of this atlas we chose a set of eighteen healthy control subjects (Macaca mulatta)in the ages from 16 to 34 months. The atlas based segmentation procedure was then applied to both the training data as well as to two additional intrauterine exposure studies with a total of over 50 additional subjects (ages 9 to 38 months). All subjects have been generated from a large 500+ monkey-breeding colony at the Harlow Primate Laboratory (HPL), with known history extending back five generations and over 25 years. Each monkey was scanned on a 3 Tesla GE scanner (SIGNA Excite) with both a high-resolution 3D-SPGR sequence (0.2344x0.2344x0.0.497976mm^3) and T2-weighted spin-echo sequence (0.2734x0.2734x1.5mm).

2.2. Atlas Building

As the first step of our segmentation framework, we determine an atlas image as the unbiased average image from a set of training images by iterative, joint deformable registration of all training datasets into a single unbiased average image[9] (see Fig 2) that has minimal deformation to all training images.

Prior to this deformable registration, the training images need to be affinely registered, skull stripped and intensity calibrated. For this purpose, in a first stage we randomly selected a training case as template and semi-automatically determined its skull-strip mask using the ITK-SNAP tool.[10] All other cases were then affinely registered[11] to this template and skull-stripped with the slightly dilated mask of the template. Using pairwise histogram quantiles matching, all images were intensity calibrated to the template. All calibrated, skull-stripped images were then voxel-wise averaged to form the initial affine average image. This affine average image was then chosen as the template and the registration, skull stripping and intensity calibration steps were repeated

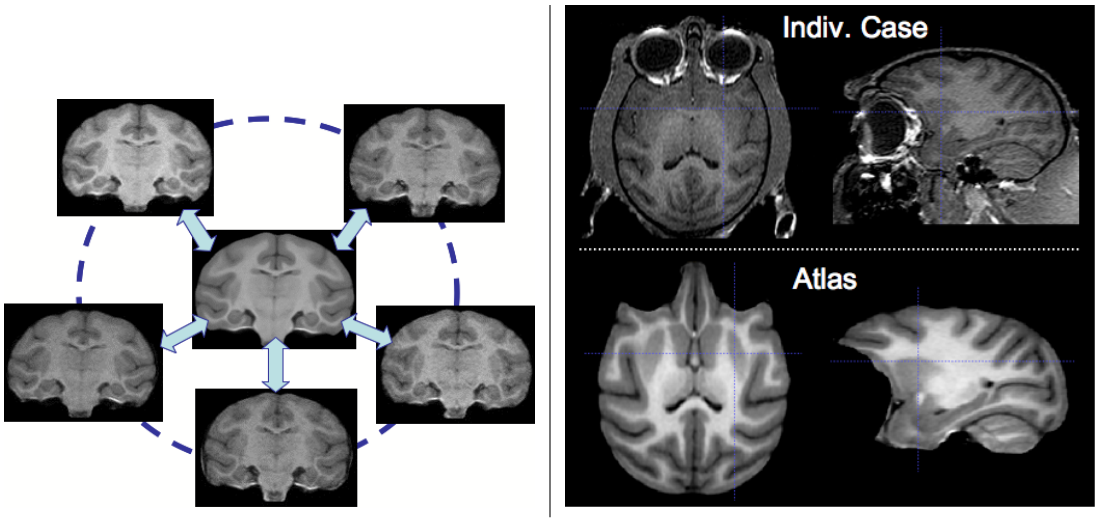

Figure 2. Left: Scheme of unbiased, average atlas image computation by jointly deforming a series of training images into their average image. Right: Computed atlas (bottom) and one of the 18 original training images at similar slices. The gain in signal to noise is clearly visible.

with the affine average template. As the final step of the atlas image computation, the unbiased deformable atlas procedure was applied to compute the final template atlas image. This atlas image represents the unbiased average that has overall minimal deformation to all training images.[9] This step was performed both for the T1 weighted and T2 weighted images, where the T2 affine average template was additionally registered to the T1 weighted image prior to the deformable atlas computation.

On this atlas image, we defined the probabilistic maps for white matter(WM), gray matter(GM) and cerebro-spinal fluid(CSF), as well traced manually the definitions of the lobar subdivisions.

The three tissue probabilistic maps were initialized with binary segmentations from manually selected thresholds: white and gray matter segmentations on the T1 image, cerebro-spinal fluid on the T2 image. These segmentations were manually edited by an expert (RK). The segmentations were slightly smoothed using a Gaussian kernel of 0.4mm variance and propagated back to the 18 affinely aligned training cases via the deformation fields computed in the atlas building. After this back propagation, the tissue segmentations were linearly averaged to form the probabilistic tissue maps. The probability maps were locally normalized to maximally 1 and a rejection class was created by subtracting the sum of all three tissue probabilities from 1.

The above described atlas image computation is based on images that have not been corrected for intensity inhomogeneity artifacts. The tissue segmentation procedure described in the next section also corrects such artifacts and thus we applied that tissue segmentation procedure to all affinely aligned training images. Both the deformable atlas image, as well as the probabilistic tissue maps were then recomputed. The final atlas image is therefore based on affinely aligned, skull stripped, intensity calibrated and intensity inhomogeneity corrected training images.

As the next step, a lobar parcellation was determined on the tissue class segmentation of the atlas by relabeling the tissues into lobes using the ITK-SNAP segmentation tool[10] for the right lobes only (rater RK). These right hemispheric definitions were mirrored at the midsagittal plane using a simple axial flip operation followed by rigid registration to produce the initial left hemispheric lobar parcellation. The initial left parcellations were then corrected using manual relabeling (RK). The full parcellation consists of separate definitions for the left and right hemisphere for the subcortical, frontal, prefrontal, cingulate, parietal, occipital, auditory, visual and limbic temporal lobes, as well as the brainstem, corpus callosum and cerebellum (see Fig. 4). The final parcellation is determined by an iterative dilation in order to fill any unlabeled areas up to 5 voxels away from the initial parcellation. As described in the next section, this lobar parcellation serves as a mask to full brain tissue segmentations.

2.3. Brain Tissue Classification and Parcellation

Automatized brain tissue classification is a common task in human neuroimaging and several solutions have been proposed (e.g.[12–15]). In our framework we employ our itkEMS tool,[15,16] which computes a probabilistic atlas based automatic tissue segmentation via an Expectation-Maximation scheme. This tool further performs an intensity inhomogeneity correction of the image that removes gradual variations in the image intensities mainly due to RF coil imperfections. The output consists of the corrected grayscale image along with binary and probabilistic maps of the tissue classes of white matter (WM), gray matter(GM), cerebrospinal fluid tissue(CSF). The binary tissue segmentations also enable a straightforward skull stripping by masking out all non-brain-tissue voxels.

The following parcellation process is computed via deformable registration of the atlas to the current image using the same fluid, diffeomophic, deformable registration process employed also in the atlas computation. The computed deformation fields are then applied to the parcellation or any other region of interest definition on the atlas.

The deformable registration process that is central to both the atlas and parcellation computation, matches directly the image intensities. Thus an appropriate intensity calibration, additional to a prior intensity inhomogeneity correction, is crucial for the computation of a high quality average image and segmentation result. Our intensity calibration method transforms all training images into the same intensity range via a spline based histogram transfer function that matches the mean intensities of the tissue classes of WM, GM and CSF, as well as the overall range of the image intensities. The mean tissue intensities are estimated using the probabilistic segmentation maps computed during the tissue classification.

In detail, our segmentation framework performs the following steps are for the computation of each individual case. First, the atlas image is affinely registered to the cases T1 image. The affine transformation is applied to the atlas probability maps and parcellation. The transformed atlas is employed in our tissue classification tool itkEMS in order to compute probabilistic and hard tissue segmentations from jointly the T1 and T2 images (see Fig. 1). This step further corrects RF-coil induced intensity non-uniformity, as well as performs brain stripping and is followed by image calibration to the atlas. Via fluid, deformable registration the transformed atlas is registered with the intensity calibrated, brain stripped images. The computed deformation field is applied to the affine transformed parcellations. These deformed parcellations mask the previously computed tissue segmentations to define the parcellation on the case (see Fig. 2).

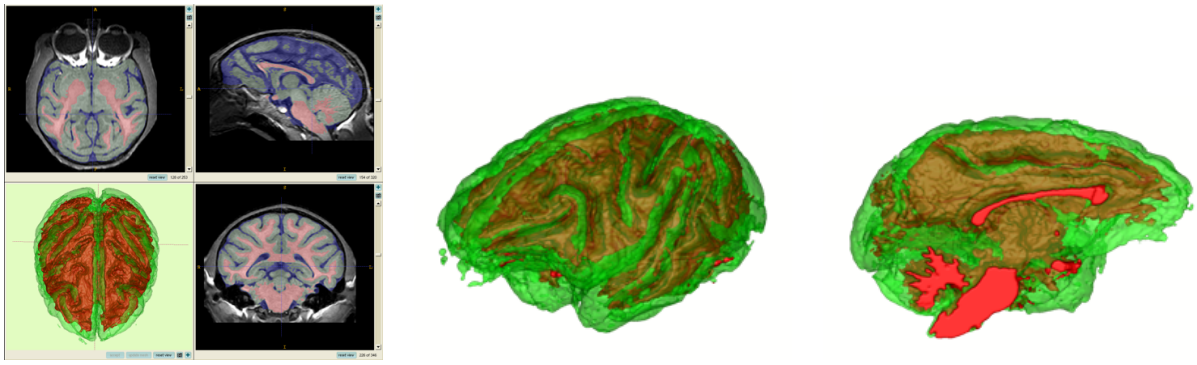

Figure 3. Visualization of a representative example of the tissue segmentation. Left: overlaid ontop of the smoothed, intensity corrected imag. Middle: 3D visualization of the white matter (red) and gray matter surface (green, transparent). Right: Medial view of segmentation after removal of right hemisphere.

3. RESULTS

We successfully built average atlas images for the T1 and T2 datasets using all 18 training datasets. The atlases clearly exhibit an enhanced signal-to-noise ratio compared to the original images (see Fig2) due to the

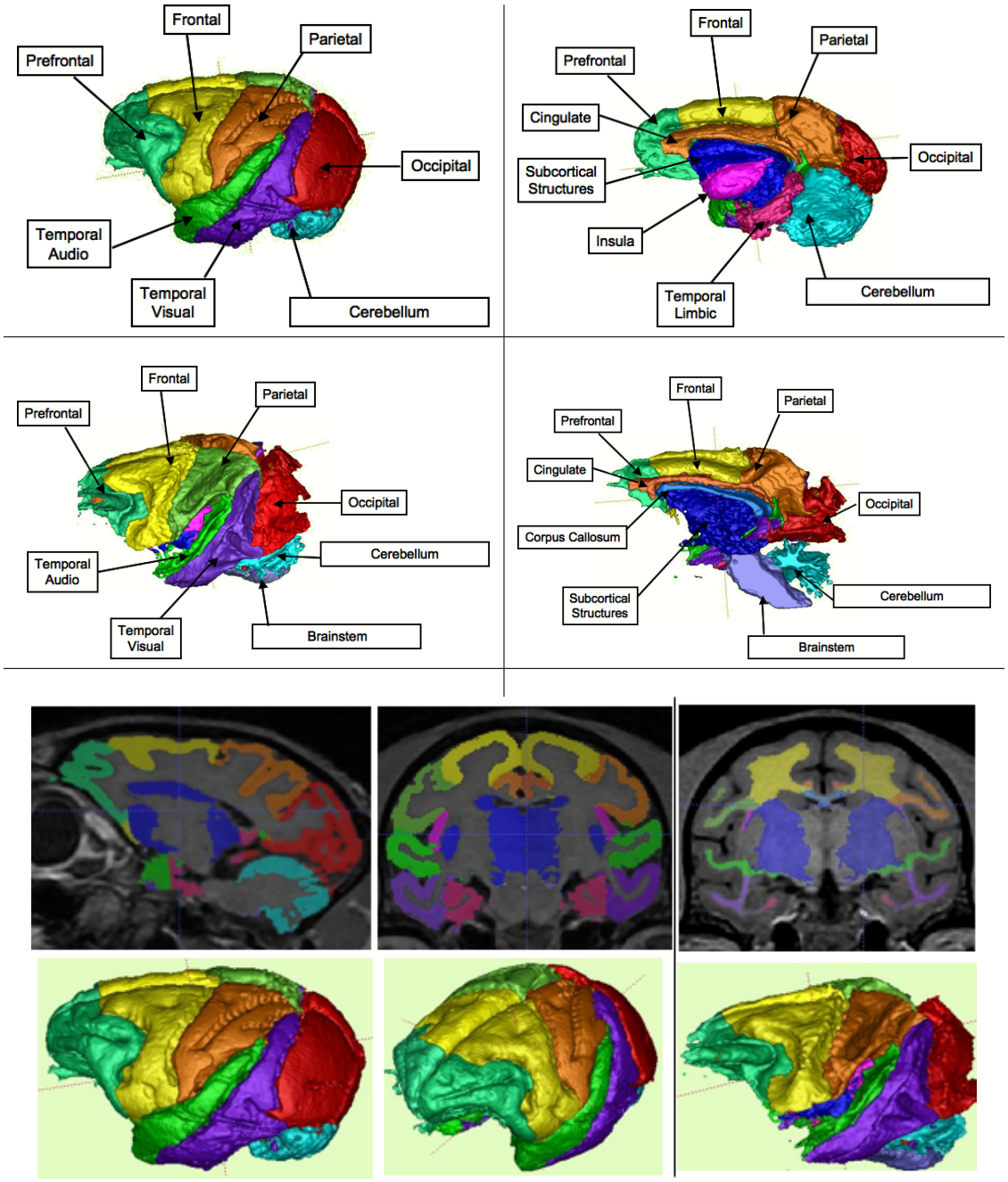

Figure 4. Visualization of the parcellation definition on a representative example of the computation. First row: gray matter parcellation. Second row: white matter structures. Third row: MR images overlaid with gray matter (left/middle) and white matter (right) parcellation. Fourth row: 3D visualizations corresponding to third row.

compaction of the corresponding intensity information from all 18 images. Furthermore, the clear definition of the cortical folds in the atlas shows that the cortical folding variability in our training set is small and highly reduced compared to human cortical folding.

The tissue segmentation was then applied to all images (see Fig. 3 for a representative case). Next, the atlas parcellation was warped into each case and the tissue segmentations were masked with the warped parcellation. Figure 4 shows the parcellated white and gray matter tissues for a representative case. The 3D renderings show how well the identification of the parcellations agrees with the sulcal locations. Especially the white matter visualization shows that the parcellation borders are located in the middle of the correct sulci.

Using the same framework, we can define regions of interest outlining the major subcortical structures on the atlas and compute the segmentation of the individual datasets (see Fig. 5A). The cortical parcellations can also be used in combination with cortical thickness measurements based on the automatic tissue segmentations (see Fig. 5B) to analyze lobar histograms of cortical thickness changes.

Even though the original atlas was build from a training population of 16-34 months of age, we have applied it successfully on datasets as young as 9 months of age. In total over 50 additional datasets have been segmented with the framework presented here without a single failure.

A: Subcortical Structure Segmentation

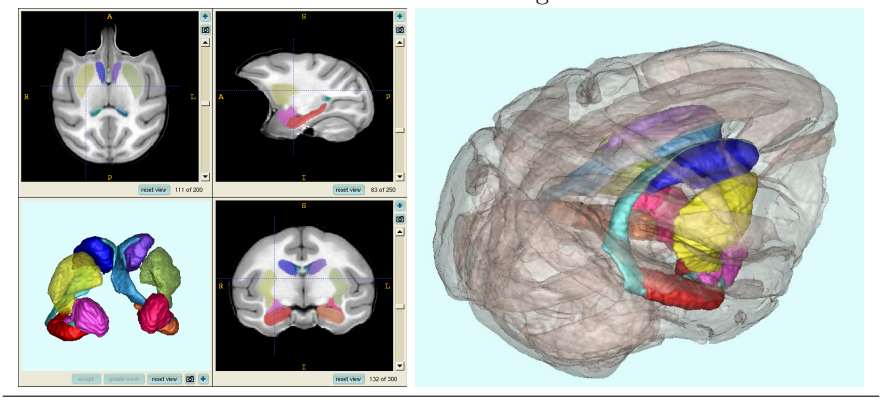

B: Cortical Thickness Analysis

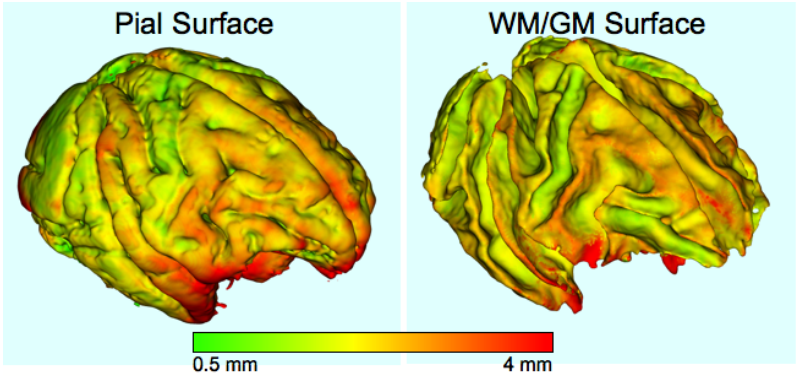

Figure 5. A: Illustration of subcortical definition on the atlas (Left: Manual definition using ITK-SNAP tool, Right: 3D Rendering with pial GM surface). B: Example of cortical thickness computation based on the automatic tissue segmentation.

4. CONCLUSION

We have presented in this work the generation and application of a rhesus monkey brain atlas for tissue classification and regional parcellation. Neither fully automatic brain tissue classification and nor automatic lobar parcellation and structural segmentation has yet been published for the analysis of rhesus monkey data.

The computed atlas image shows that the cortical variability in our training data is highly limited. The deformable registration is able to identify corresponding cortical gyri accurately in the atlas, its training datasets as well as additional unrelated datasets.

The individual methods used in the segmentation pipeline have been applied before on human data, but their combination is novel, as is their adaptation and application to rhesus monkey MRI data. Furthermore, we generated a novel, high-resolution rhesus monkey atlas with high signal-to-noise ratio. The atlas is appropriate for the intermediate developmental stages up to early adult age.

5. ACKNOWLEDGMENT

This research has is supported by the UNC Neurodevelopmental Disorders Research Center HD 03110 as well as the NIH AI067518 (Maternal flu infection and brain development in primates).

REFERENCES

1. H. A. Drury, D. C. V. Essen, C. H. Anderson, C. W. Lee, T. A. Coogan, and J. W. Lewis, "Computerized mappings of the cerebral cortex: a multiresolution flattening method and a surface-based coordinate system," *Journal of cognitive neuroscience* **8**(1), pp. 1–28, 1996.
2. D. Van Essen, H. Drury, S. Joshi, and M. Miller, "Comparisons between human and macaque using shape-based deformation algorithms applied to cortical flat maps," in *3rd Int. Conference on Functional Mapping of the Human Brain*, p. S41., 1997.
3. M. M. Adams, P. R. Hof, R. Gattass, M. J. Webster, and L. G. Ungerleider, "Visual cortical projections and chemoarchitecture of macaque monkey pulvinar," *The Journal of comparative neurology* **419**, pp. 377–93, Apr. 2000.
4. D. C. V. Essen, J. W. Lewis, H. A. Drury, N. Hadjikhani, R. B. Tootell, M. Bakircioglu, and M. I. Miller, "Mapping visual cortex in monkeys and humans using surface-based atlases," *Vision research* **41**(10-11), pp. 1359–78, 2001.
5. D. C. V. Essen, "Surface-based atlases of cerebellar cortex in the human, macaque, and mouse," *Annals of the New York Academy of Sciences* **978**, pp. 468–79, Dec. 2002.
6. D. C. V. Essen, "Surface-based approaches to spatial localization and registration in primate cerebral cortex," *NeuroImage* **23 Suppl 1**, pp. S97–107, 2004.
7. K. L. Narr1, R. P. Woods, P. M. Thompson, P. Szeszko, D. Robinson, T. Dimtcheva, M. Gurbani, A. W. Toga, and . Robert M. Bilder2, "Relationships between iq and regional cortical gray matter thickness in healthy," *Cereb Cortex* , November 2006.
8. N. Makris, J. Kaiser, C. Haselgrove, L. J. Seidman, J. Biederman, D. Boriel, E. M. Valera, G. M. Papadimitriou, B. Fischl, V. S. C. Jr., and D. N. Kennedy, "Human cerebral cortex: A system for the integration of volume- and surface-based representations," *NeuroImage* **33**, pp. 139 – 153, 2006.
9. S. Joshi, B. Davis, M. Jomier, and G. Gerig, "Unbiased diffeomorphic atlas construction for computational anatomy," *NeuroImage* **23**, pp. S151–S160, 2004.
10. P. Yushkevich, J. Piven, H. Cody Hazlett, R. Gimpel Smith, S. Ho, J. Gee, and G. Gerig, "User-guided 3d active contour segmentation of anatomical structures: Significantly improved efficiency and reliability," *NeuroImage* **31**, pp. 1116 – 1128, 2006.
11. D. Rueckert, A. Frangi, and J. Schnabel, "Automatic construction of 3d statistical deformation models using non-rigid registration," in *MICCAI*, pp. 77–84, 2001.
12. W. Wells, W. Grimson, R. Kikinis, and F. Jolesz, "Adaptive Segmentation of MRI Data," *IEEE Trans. Med. Imaging* **15**, pp. 429–443, August 1996.

13. K. Van Leemput, F. Maes, D. Vandermeulen, and P. Suetens, "Automated model-based bias eld correction of mr images of the brain," *IEEE Transactions on Medical Imaging* **18**(10), pp. 885–896, 1999.
14. D. Pham and J. Prince, "An adaprive fuzzy segmentation for three-dimensional magnetic resonance images," in *Proc. of Information Processing in Medical Imaging, IPMI 99*, *Lecture Notes in Computer Science*(1613), pp. 140–153, Springer, 1999.
15. M. Styner, H. C. Charles, J. Park, J. Lieberman, and G. Gerig, "Multi-site validation of image analysis methods - assessing intra and inter-site variability," in *SPIE Medical Imaging*, **4684**, pp. 278–286, 2002.
16. M. Prastawa, J. H. Gilmore, and W. L. andGuido Gerig, "Automatic segmentation of mr images of the developing newborn brain," *Medical Image Analysis* **9**, pp. 457–466, October 2005.